Omnidirectional Au-Embedded ZnO/CdS Core/Shell Nanorods for Enhanced Photoelectrochemical Water-Splitting Efficiency

SUPPORTING INFORMATION

Experimental procedures

Preparation of ZnO nanofibers. ZnO nanofibers (NFs) were fabricated by electrospinning (ES) method using a TL nanofiber electrospinning equipment (Tong Li Tech). Zinc acetate dihydrate ($Zn[CH_3COO]_2.2H_2O$, Merck 99.8%) was used as the precursor and polyvinylpyrrolidone (PVP, MW = 360000 g/mol) as the template for the preparation of ES solution. Initially, PVP (16.7 wt.%) was dissolved in the solvent consisting of ethanol and N,N-dimethyl-formamide (DMF) with a volume ratio of 3:1. The solution was constantly stirred using a magnetic stirrer at room temperature for 1 hour. In the next step, 1.09 g of zinc acetate dihydrate was added into the solution, which was then further stirred for 1 hour.

The ITO substrate with the dimensions of 1 cm $\times$ 2 cm was immobilized on the cathode, whereas the syringe pump was connected to the anode. A high-voltage of 10 kV was applied between the anode and the cathode. The distance between the syringe needle and the substrate was fixed at 12 cm. The solution was injected at a rate of 0.02 mL/h, resulting in the formation of Zn-PVP nanofibers on the ITO substrate (Zn-PVP NFs/ITO). The injection time was varied to change the thickness of the NFs layer. The samples were then annealed in air at 500 °C for 2 h to remove PVP that eventually formed ZnO NFs/ITO substrates.

Hydrothermal growth of omnidirectional ZnO nanorods. The ZnO NFs/ITO substrates obtained from the ES method were used as the substrates for the fabrication of omnidirectional ZnO nanorods (ZnO NRs). In this process, an aqueous solution of zinc nitrate [$Zn(NO_3)_2.6H_2O$] and hexamethylenetetramine ($C_6H_{12}N_4$) (volume ratio of 1:1)

with a molar concentration of 0.04 M was prepared. The substrates were immersed in the solution contained in a stainless steel autoclave (volume of 100 ml). The hydrothermal growth was carried out at 90 °C for different growth times (i.e., 1, 3, 4 and 6 h).

Deposition of Au nanoparticles (NPs) on ZnO NRs. Photoreduction method was used to deposit Au NPs on the surface of ZnO NRs.[1] Firstly, 1 mL of aqueous $HAuCl_4$ 0.5 mM (Sigma-Aldrich) and 0.02 g PVP were dispersed in 50 mL of ethanol in a Pyrex Petri dish to prepare the Au^{3+} precursor. Then, the ZnO NRs on ITO substrates were immersed in the dish, followed by an irradiation under UV light generated by an UV lamp (25 W) for various times (i.e., 30, 60 and 180 s) to reduce Au^{3+} ions into Au^0. After the irradiation, the substrates were washed in ethanol to remove the PVP. Finally, the samples were dried at in air at 60 °C.

Preparation of Au NPs-embedded ZnO/CdS core/shell heterostructures. CdS shell was grown on the surface of ZnO/Au NRs via the chemical bath deposition (CBD) method by soaking the substrates in the aqueous solution containing $Cd(NO_3)_2.4H_2O$ 10 mM and C_2H_5NS 10 mM at room temperature for 30 min. The substrates were then rinsed with DI water and dried at room temperature in N_2 ambient.

The fabrication processes of the nanostructures are summarized as in Fig. S1.

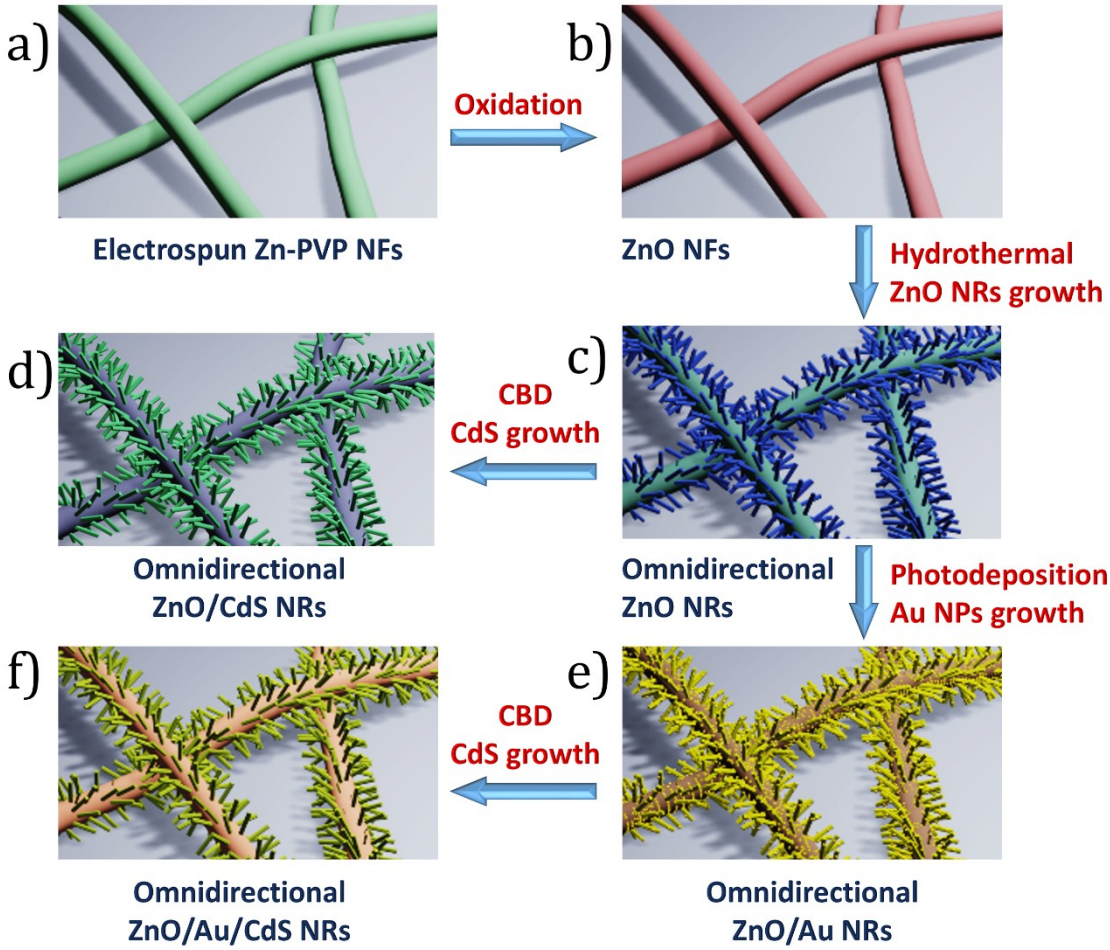

Fig. S1. The process flow for the fabrication of omnidirectional ZnO/Au/CdS NRs.

Characterization of the nanostructures. The crystalline structure of the nanostructures was examined by X-ray diffraction technique using a Siemens D5005 diffractometer equipped with a Cu Kα radiation source. The morphology of the nanostructures was investigated by scanning electron microscopy and transmission electron microscopy using a Hitachi S4800 and a JEOL-JEM 2100F, respectively. The UV-VIS absorption spectra were recorded using a SCINCO S-3100 spectrophotometer.

Determination of Au concentration. The concentration of Au as a function of growth time was determined by ICP-OES method, using an ICP-OES Icap 6000 (Thermo Scientific). The ZnO/Au/CdS nanorods were peeled off from the substrate and dissolved in the solution containing HCl(30%), HNO_3(60%) and HF(40%) with a volume ratio of 9:3:1,

which was then destructed using microwave for 2 hours. Hereafter, the sample was washed in MQ water and analyzed with ICP-OES to measure the concentration of Au.

Photoelectrochemical measurements. The photoelectrochemical (PEC) water-splitting performance of the materials was investigated using a 4-electrode electrochemical analyzer (Model DY2300). The substrates with the obtained nanostructures were used as the working electrode, whereas Pt-foil and Ag/AgCl in saturated KCl were used as the as the counter and the reference electrodes, respectively. For the ZnO nanostructures without CdS and Au, Na_2SO_4 solution (0.5 M) was used as the electrolyte; for other heterostructures, the electrolyte was the mixture of Na_2S solution (0.25 M) and Na_2SO_3 (0.35 M). A 150 W Xe lamp with a flux of 75 $mW \cdot cm^{-2}$ was used as the light source. The potential was swept linearly at a scan rate of 10 $mV \cdot s^{-1}$. The photoconversion efficiency is calculated using the equation:[2]

$$\eta(\%) = J_p(E_{rev} - E_{app})*100/I_o \quad (1)$$

Where J_p is photocurrent density ($mA \cdot cm^{-2}$), I_o is the power density of incident light, E_{rev} is the standard state-reversible potential (which is 1.23 V *vs.* NHE), and E_{app} is the applied potential, which is calculated by $E_{app} = E_{meas} - E_{aoc}$, in which E_{meas} is the electrode potential (vs. Ag/AgCl) of the working electrode at which photocurrent was measured under illumination, and E_{aoc} is the electrode potential (vs. Ag/AgCl) of the same working electrode under open circuit conditions.[2]

Fig. S2 shows XRD patterns of the Zn-PVP NFs, ZnO NFs and the omnidirectional ZnO NRs. For the as-deposited Zn-PVP NFs, only the diffraction peaks of the ITO substrates were found. The signature of the crystalline ZnO only appeared after the annealing, which is represented by the peaks at 31.8, 34.5, 36.3, 47.6, and 56.6°. These peaks arise from the diffraction on the (100), (002), (101), (102) and (110), respectively, of the wurtzite structure.[3] After the hydrothermal growth of the ZnO NRs, the intensity of the (002) peak increased significantly in comparison with the intensities of the other peaks, suggesting the *c*-axis preferential orientation growth of the ZnO NRs.

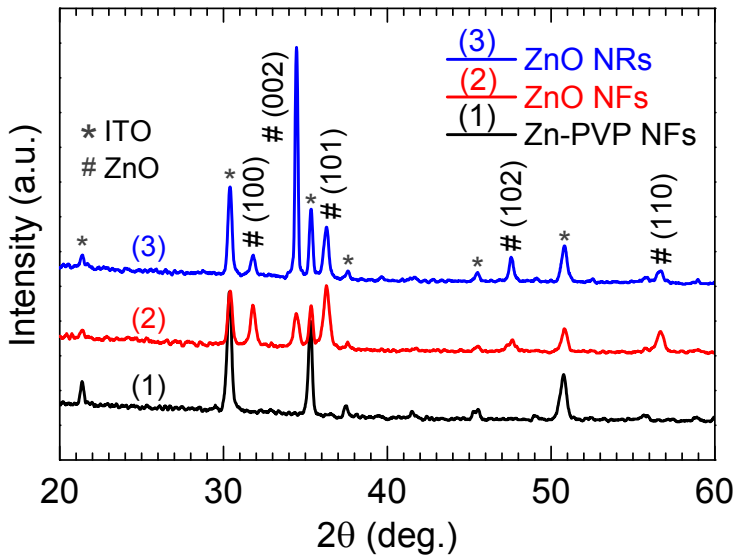

Fig. S2. XRD patterns of as-deposited Zn-PVP NFs (1), ZnO NFs obtained after the oxidation of Zn-PVP NFs at 500 °C in air for 2 h (2) and the omnidirectional ZnO NRs obtained by hydrothermal growth at 90 C for 4 h (3).

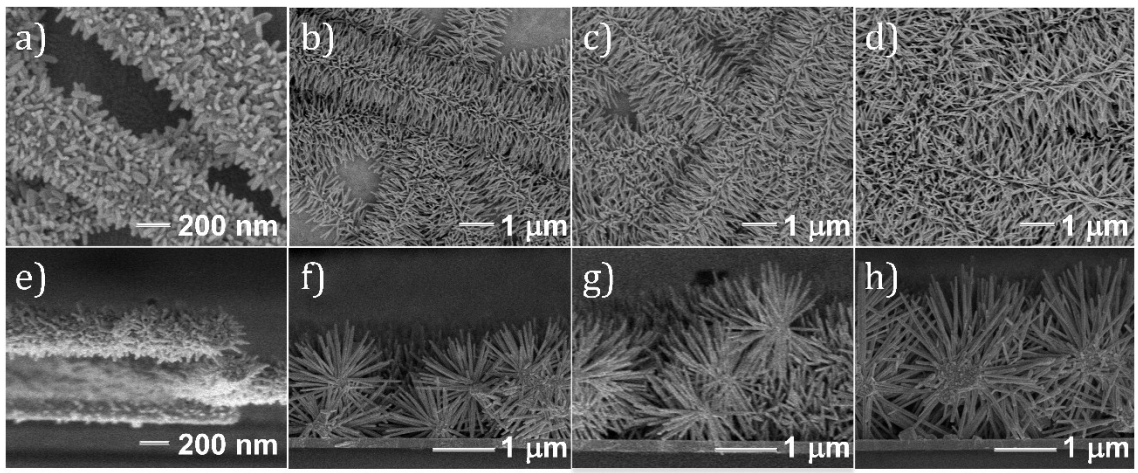

Fig. S3. SEM images showing the planar view (top) and cross-sectional view (bottom) of the omnidirectional ZnO NRs for different growth times: 1 h (a & e), 3 h (b & f), 4 h (c & g) and 6h (d & h).

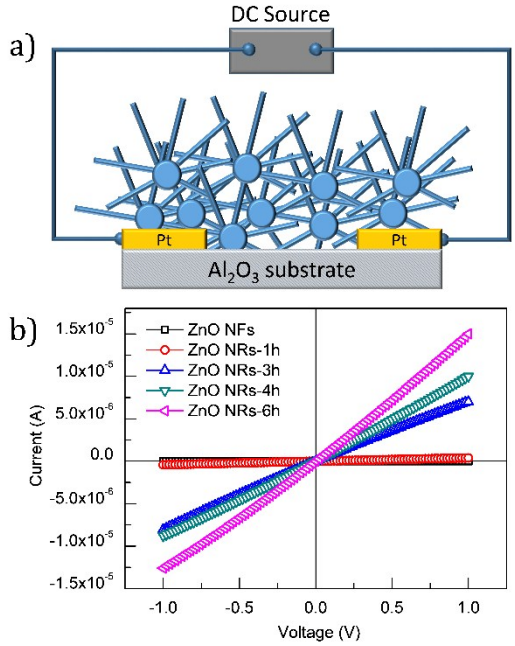

Fig. S4. Circuit configuration of the electrical structure for measuring the electrical conductivity of the omnidirectional ZnO NRs (a) and the current – voltage (I – V) characteristics obtained for the ZnO NFs and the omnidirectional structures with different NRs growth times from 1 to 6 h (b). We note that the results obtained from this electrical measurement only reflect the improved electrical conductivity between the NRs on the top layer and does not represent the improved electrical conductivity between the sensitized layer and the substrate. The latter can be achieved by using AC impedance method, which has not been investigated in this work. Nevertheless, from the cross-sectional SEM images presented in Figure S3e – h, we observed that with increasing ZnO NRs growth time, more contacts between ZnO NRs and the substrate were created. Therefore, we believe that the electrical contact between the top layer and the substrate was improved.

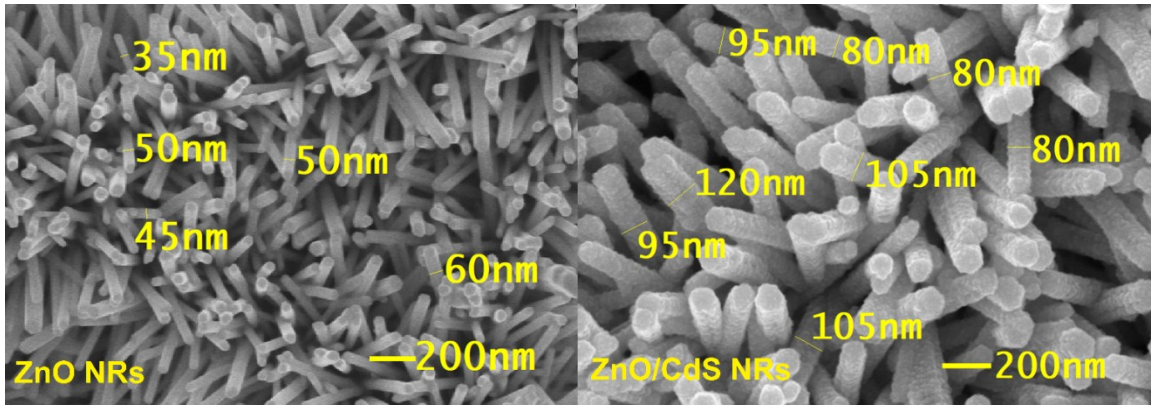

Fig. S5. SEM images of ZnO NRs (left) and ZnO/Au/CdS NRs (right) and the measured diameters. The diameter of the ZnO NRs is in the range of 40 – 70 nm; the diameter of the ZnO/CdS NRs is in the range of 80 – 130 nm. By comparing the diameter of the NRs before and after coating with the CdS layer, the thickness of the CdS layer was estimated, which is in the range of 20 – 30 nm. This is consistent with the diameter measured by TEM, as presented in Fig. S6.

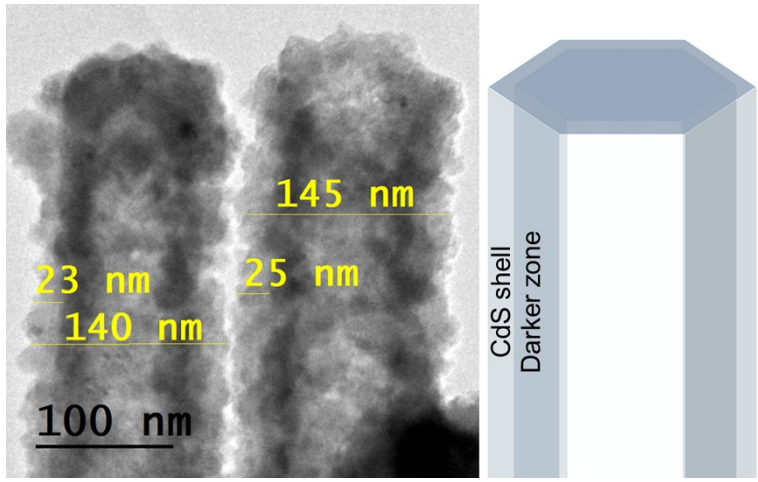

Fig. S6. TEM image of ZnO/CdS NRs (left) and a schematic drawing (right) that was used to explain the contrast between the areas on the TEM image and how the thickness of the CdS layer was measured.

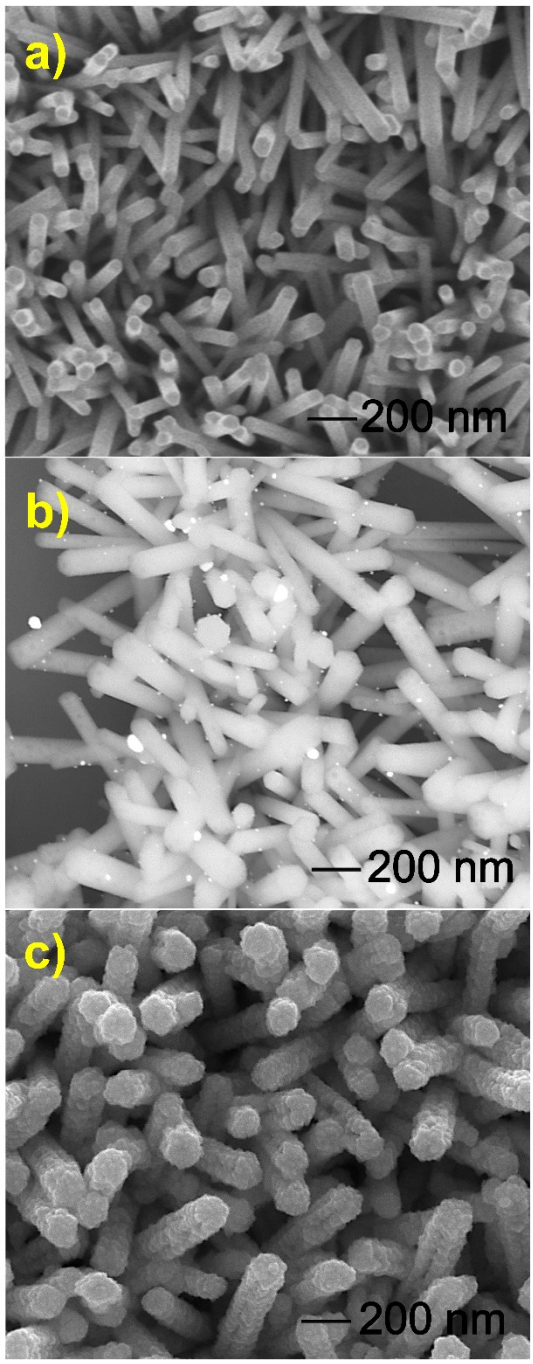

Fig. S7. SEM images of ZnO NRs (a), ZnO/Au NRs (b) and ZnO/Au/CdS NRs (c). The ~~A~~ ZnO/Au/CdS NRs were fabricated by first depositing Au nanoparticles onto ZnO NRs. Hereafter, the CdS layer was grown to form the core/shell structure. The SEM image of ZnO/Au NRs exhibits the presence of Au NPs, which are not found on the surface of ZnO/Au/CdS NRs. This is evident that Au NPs are embedded between ZnO and CdS.

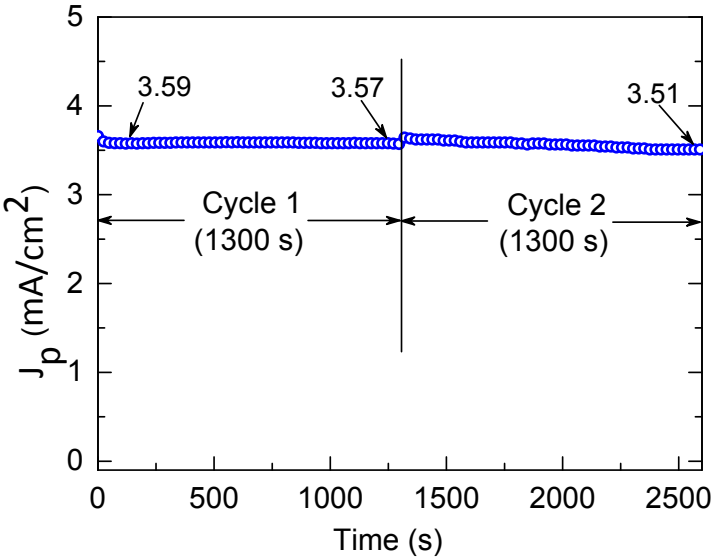

Fig. S8. The stability of the current density under continuous irradiation. A drop of 2.2% was observed after a total irradiation of 2600 s (2 cycles).

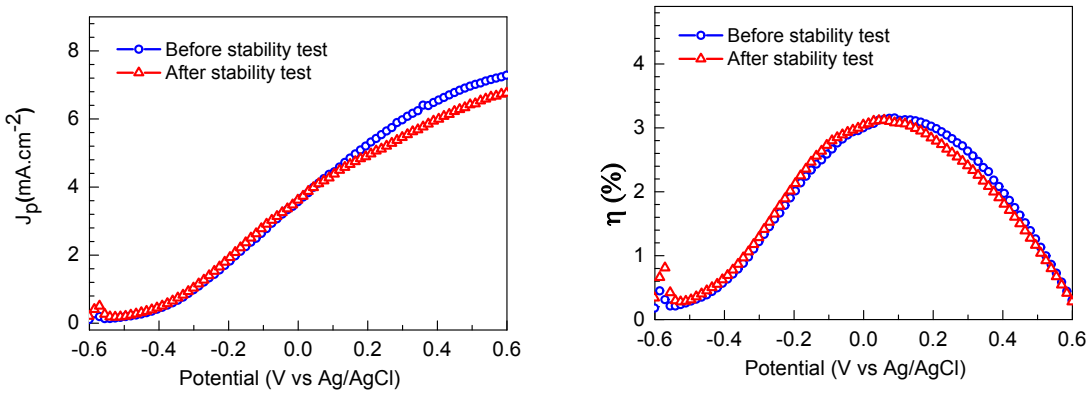

Fig. S9. Photocurrent density (left) and photoconversion efficiency (right) curves measured on the ZnO/Au/CdS (60 s Au growth time or 1.2% Au) before and after two cycles of stability test (i.e., in total 2600 s).

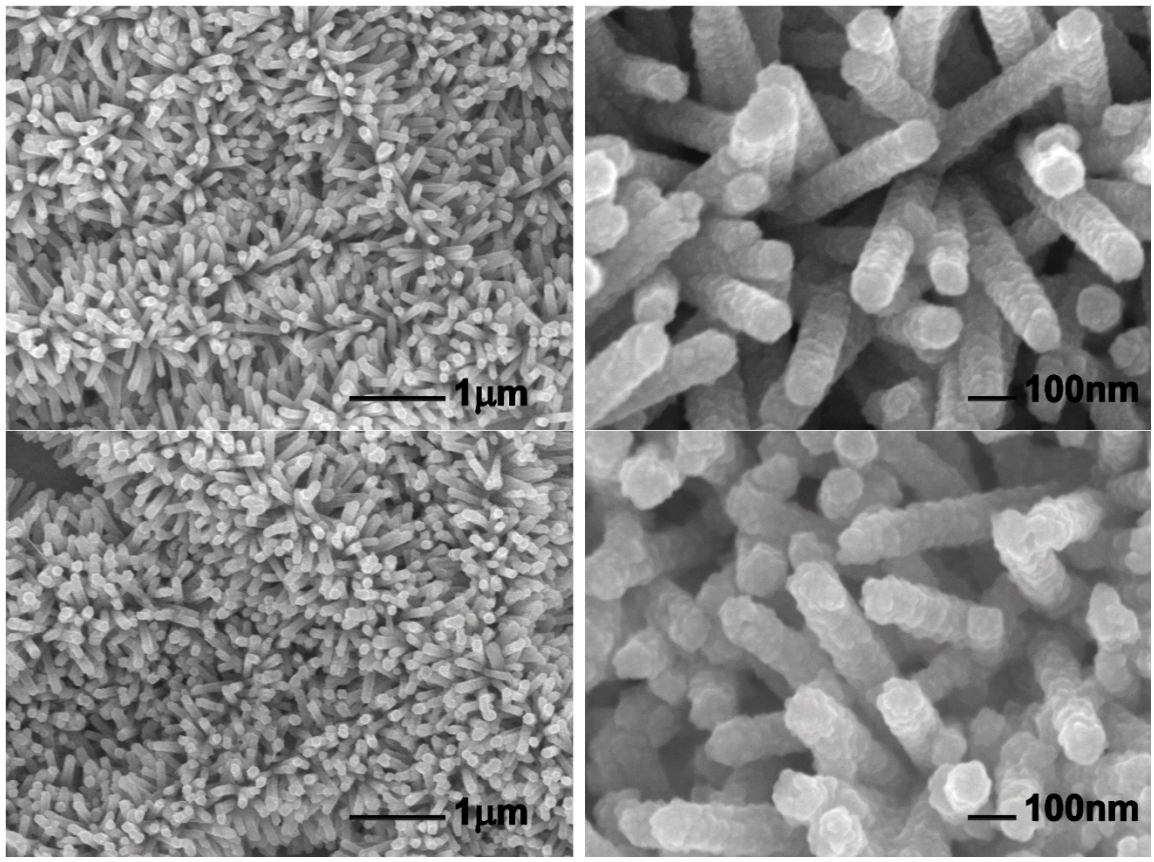

Fig. S 10. SEM images (at magnifications of 20K (the left images) and 100K (the right images)) of ZnO/Au/CdS structure before (top) and after (right) water-splitting stability test.

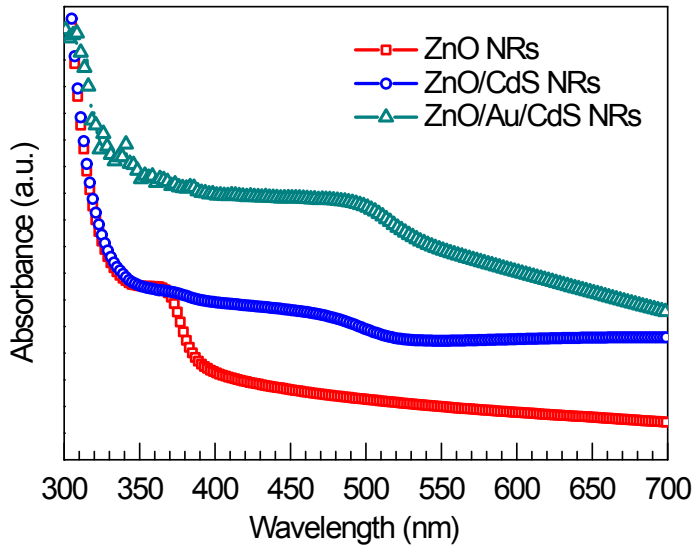

Fig. S11. UV-Vis absorption spectra of ZnO NRs, ZnO/CdS NRs and Au-embedded ZnO/CdS NRs. The results indicate that the coating of CdS enabled the absorption of light in the visible region, which was further enhanced by Au NPs.

References

1 F. Xu, J. Mei, M. Zheng, D. Bai, D. Wu, Z. Gao and K. Jiang, *J. Alloys Compd.*, 2017, **693**, 1124–1132.

2 S. U. M. Khan, M. Al-Shahry and W. B. Ingler, *Science (80-.).*, 2002, **297**, 2243–2245.

3 C. Li, T. Ahmed, M. Ma, T. Edvinsson and J. Zhu, *Appl. Catal. B Environ.*, 2013, **138–139**, 175–183.